

## Optical properties of the antiperovskite superconductor $\text{MgCNi}_3$

This article has been downloaded from IOPscience. Please scroll down to see the full text article.

2003 J. Phys.: Condens. Matter 15 833

(<http://iopscience.iop.org/0953-8984/15/6/310>)

View [the table of contents for this issue](#), or go to the [journal homepage](#) for more

Download details:

IP Address: 171.66.16.119

The article was downloaded on 19/05/2010 at 06:33

Please note that [terms and conditions apply](#).

# Optical properties of the antiperovskite superconductor $\text{MgCNi}_3$

C M I Okoye<sup>1</sup>

The Abdus Salam International Centre for Theoretical Physics, Trieste, Italy

E-mail: okoyecmi@yahoo.com

Received 6 September 2002, in final form 4 December 2002

Published 3 February 2003

Online at [stacks.iop.org/JPhysCM/15/833](http://stacks.iop.org/JPhysCM/15/833)

## Abstract

The optical properties of the antiperovskite superconductor  $\text{MgCNi}_3$  have been calculated using the full-potential linearized augmented-plane-wave method within the generalized gradient approximation scheme for the exchange–correlation potential. In order to fully elucidate the optical properties of  $\text{MgCNi}_3$ , the dielectric function  $\varepsilon(\omega)$ , the reflectivity  $R(\omega)$ , the optical absorption coefficient  $I(\omega)$ , the optical conductivity  $\sigma(\omega)$ , the energy-loss function  $L(\omega)$ , the refractive index  $n(\omega)$  as well as the extinction coefficient  $k(\omega)$  were calculated. The prominent features in the spectra of the optical parameters are discussed.

## 1. Introduction

Recently, a new intermetallic superconductor,  $\text{MgCNi}_3$ , was discovered by He *et al* [1] with the transition temperature  $T_c \sim 8$  K, the first for a material which has the perovskite structure without any oxygen. Interest in this compound arose not because of its relatively low transition temperature but rather as a result of the high proportion of Ni in the compound which suggests that magnetic interactions may be important to the existence of the superconductivity and hence makes it a potential candidate for exhibiting unconventional superconductivity. Surprisingly, no magnetic or structural transitions have been found in  $\text{MgCNi}_3$  in the range 2–295 K [2]. On doping with Cu (electron doping) on the Ni site,  $T_c$  decreases systematically, but with Co doping (hole doping), the superconductivity disappears abruptly for doping of only 1% [3] and there is no evidence that the quenching of superconductivity is related to magnetism.

$\text{MgCNi}_3$  has the cubic antiperovskite structure. It is called an antiperovskite structure because the transition metals are located at the corners of the octahedron cage in contrast to the ordinary perovskite structure [4]. According to refinements [1],  $\text{MgCNi}_3$  is stoichiometric with only a very small, 4%, carbon deficiency and occurs in the cubic antiperovskite structure. There are some recent electronic structure studies of this compound [3, 5–9] but there has been

<sup>1</sup> Permanent address: Department of Physics and Astronomy, University of Nigeria, Nsukka, Nigeria.

no study yet of the optical properties. The study of the optical properties is important because it helps to give some insight into the electronic structure.

Recently, first-principles methods have been employed in the study of the optical properties of perovskites [10–15]. In this paper, we shall use the generalized gradient approximation (GGA) within the well established full-potential linearized augmented-plane-wave (FP-LAPW) method [16, 17] to study the optical properties of the superconducting antiperovskite  $\text{MgCNi}_3$ . The calculational procedure will be presented in section 2. Section 3 will be devoted to the presentation and discussion of the results and conclusions are drawn in section 4.

## 2. Method of calculation

We have carried out self-consistent calculations using the FP-LAPW method for cubic antiperovskite  $\text{MgCNi}_3$  at the experimental lattice constant of  $a = 3.82 \text{ \AA}$  [8]. In this calculational scheme, there are no shape approximations to the charge density or potential. The calculations are based on the GGA to the density functional theory [18, 19] with the exchange–correlation potential parametrized according to the Perdew–Burke–Ernzerhof scheme (PBE-GGA) [20]. In the FP-LAPW method, the unit cell is divided into two parts: non-overlapping atomic spheres (centred at atomic sites) and an interstitial region. The sphere radii used in the calculations for Mg, C and Ni are 1.5, 1.4 and 2.0 au respectively. Within these spheres, the potential is expanded in the form

$$V(r) = \sum_{lm} V_{lm}(r) Y_{lm}(\hat{r}) \quad (1)$$

and outside the sphere

$$V(r) = \sum_{\mathbf{K}} V_{\mathbf{K}} \exp^{i\mathbf{K}r} \quad (2)$$

where  $Y_{lm}(\hat{r})$  is a linear combination of radial functions times spherical harmonics.

For the calculation of the optical properties, a dense mesh of uniformly distributed  $k$ -points is required. Hence, the Brillouin zone integration was performed using the tetrahedron method with 560  $k$ -points in the irreducible part of the Brillouin zone without broadening. Well converged solutions were obtained for  $R_{MT} K_{max} = 8$ , where  $R_{MT}$  is the smallest of all atomic sphere radii and  $K_{max}$  is the plane-wave cut-off. The dielectric function ( $\varepsilon(\omega) = \varepsilon_1(\omega) + i\varepsilon_2(\omega)$ ) is known to describe the optical response of the medium at all photon energies  $E = \hbar\omega$ . The interband contribution to the imaginary part of the dielectric function  $\varepsilon(\omega)$  is calculated by summing transitions from occupied to unoccupied states (with fixed  $\mathbf{k}$ ) over the Brillouin zone, weighted with the appropriate matrix elements giving the probability for the transition. Specifically, in this study, the imaginary part of the dielectric function  $\varepsilon(\omega)$  is given as in [21] by

$$\varepsilon_2(\omega) = \left( \frac{4\pi^2 e^2}{m^2 \omega^2} \right) \sum_{i,j} \int \langle i|M|j \rangle^2 f_i(1 - f_j) \delta(E_f - E_i - \omega) d^3k \quad (3)$$

where  $M$  is the dipole matrix,  $i$  and  $j$  are the initial and final states respectively,  $f_i$  is the Fermi distribution function for the  $i$ th state, and  $E_i$  is the energy of electron in the  $i$ th state. The real part ( $\varepsilon_1(\omega)$ ) of the dielectric function can be extracted from the imaginary part using the Kramers–Kronig relation in the form [21, 22]

$$\text{Re}[\varepsilon(\omega)] = \varepsilon_1(\omega) = 1 + \frac{2}{\pi} \text{P} \int_0^\infty \frac{\omega' \varepsilon_2(\omega') d\omega'}{(\omega'^2 - \omega^2)} \quad (4)$$

where P implies the principal value of the integral.

The knowledge of both the real and imaginary parts of the dielectric tensor allows the calculation of important optical functions. In this paper, we present and analyse the reflectivity  $R(\omega)$ , the absorption coefficient  $I(\omega)$ , the optical conductivity  $\sigma(\varepsilon)$ , the electron energy-loss spectrum  $L(\omega)$ , as well as the refractive index  $n(\omega)$  and the extinction coefficient  $k(\omega)$ . The reflectivity spectra are derived from Fresnel's formula for normal incidence assuming an orientation of the crystal surface parallel to the optical axis using the relation [23]

$$R(\omega) = \left| \frac{\sqrt{\varepsilon(\omega)} - 1}{\sqrt{\varepsilon(\omega)} + 1} \right|^2. \quad (5)$$

We calculate the absorption coefficient  $I(\omega)$ , the real part of optical conductivity  $\text{Re}[\sigma(\omega)]$  and the electron energy-loss spectrum  $L(\omega)$  using the following expressions [23, 24]:

$$I(\omega) = \sqrt{2}(\omega) \left( \sqrt{\varepsilon_1(\omega)^2 + \varepsilon_2(\omega)^2} - \varepsilon_1(\omega) \right)^{1/2}, \quad (6)$$

$$\text{Re}[\sigma(\omega)] = \frac{\omega \varepsilon_2}{4\pi} \quad (7)$$

$$L(\omega) = \frac{\varepsilon_2(\omega)}{\varepsilon_1(\omega)^2 + \varepsilon_2(\omega)^2}. \quad (8)$$

The optical spectra such as the refractive index,  $n(\omega)$ , and the extinction coefficient,  $k(\omega)$ , are also easily calculated in terms of the components of the complex dielectric function as follows [23]:

$$n(\omega) = \left[ \frac{\varepsilon_1(\omega)}{2} + \frac{\sqrt{\varepsilon_1(\omega)^2 + \varepsilon_2(\omega)^2}}{2} \right]^{1/2} \quad (9)$$

$$k(\omega) = \left[ \frac{\sqrt{\varepsilon_1(\omega)^2 + \varepsilon_2(\omega)^2}}{2} - \frac{\varepsilon_1(\omega)}{2} \right]^{1/2}. \quad (10)$$

### 3. Results and discussion

In order to fully interpret the optical spectra which arise from interband transitions, we briefly describe the electronic properties of MgCNi<sub>3</sub>. The Brillouin zone integration for the ground state properties was performed using 1000  $k$ -points in the whole Brillouin zone. Fitting of the Murnaghan equation of state [25] to the total energies versus lattice volume yields the equilibrium lattice constant ( $a_{eq}$ ) = 7.234 au, the bulk modulus ( $B_0$ ) = 172.2 GPa and the pressure derivative of the bulk modulus ( $B'$ ) = 4.768. When the equilibrium lattice constant is compared with the experimental value, we find a 0.6% overestimation.

The electronic band structure along the high-symmetry directions of the simple cubic Brillouin zone is shown in figure 1. It is seen that MgCNi<sub>3</sub> is metallic with the Fermi level  $E_F$  lying within the valence band. The two bands that cross the Fermi level are the antibonding Ni  $d_{xz}$ ,  $d_{yz}$  orbitals which also hybridize with the C  $p$  orbital especially between the X point through the M point to the  $\Gamma$  point. They lie between  $-0.5$  and  $1.5$  eV in fair agreement with the results in [5]. Below the Fermi level the bands consist of hybridized Ni 3d and C 2p bands but with predominantly Ni 3d character. The lowest-lying band is a broad carbon 2s band with width of about 2 eV between  $-13.0$  and  $-11.0$  eV. This band is separated from the rest of the valence band by a wide gap. The lowest valence band has a minimum at the R point and has a mixture of C  $p$  and Ni  $d$  character.

Figures 2–7 show the optical functions of MgCNi<sub>3</sub> calculated for photon energies up to 12 eV. The study of the optical functions helps to give a better understanding of the

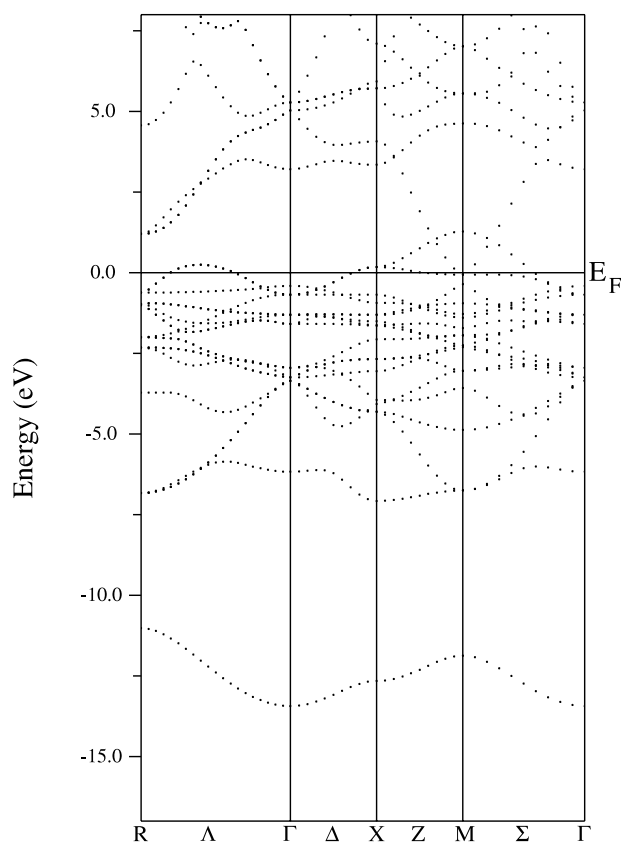
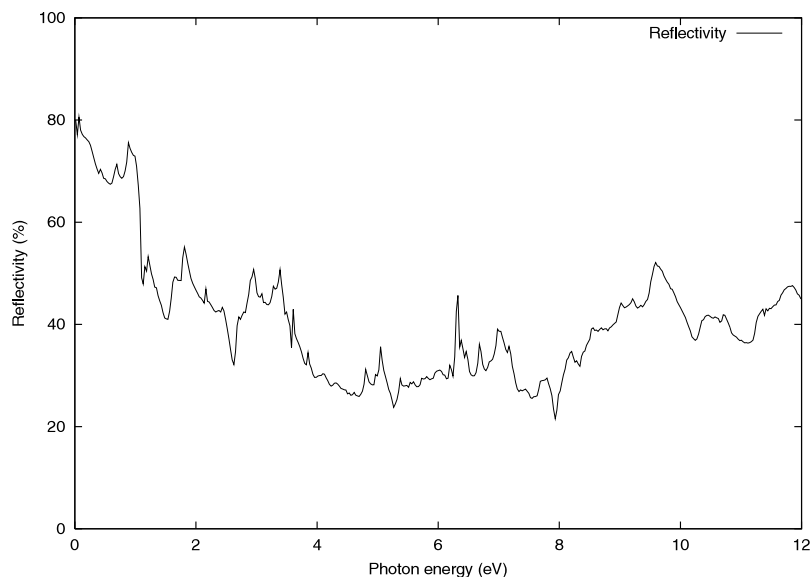


**Figure 1.** Electronic band structures of  $\text{MgCNi}_3$ .

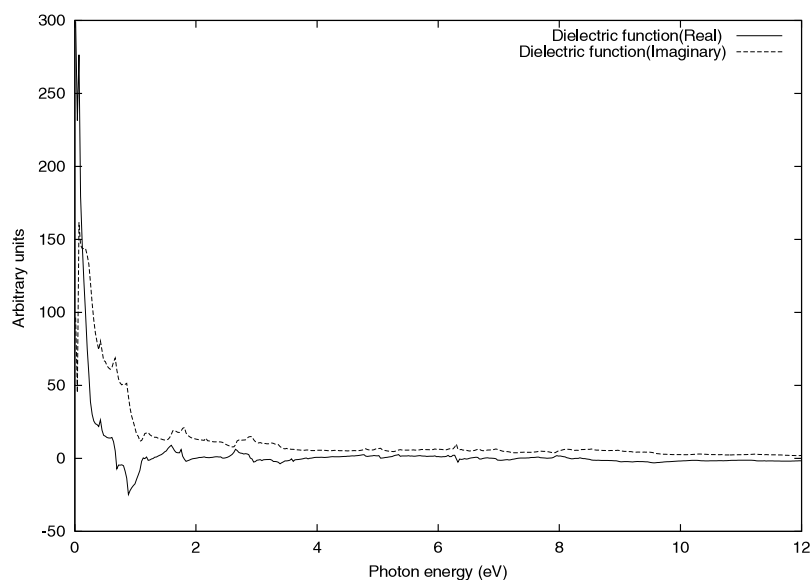
electronic structure. It is noted that for the interpretation of optical spectra, it may not be realistic to give single-transition assignments to peaks present in a spectrum since many transitions, both direct and indirect, may be found in the band structure with an energy corresponding to the peak [10, 15].

Figure 2 shows the reflectivity of  $\text{MgCNi}_3$  as a function of photon energy calculated using equation (5). We notice that the reflectivity is over 70% in the region up to  $\sim 1.0$  eV, then drops off to about 40% and subsequently exhibits some peaks at higher energies probably as a result of interband transitions.

The imaginary and real parts of the dielectric function calculated using equations (3) and (4) are displayed in figure 3. It is observed that the real part of the dielectric function vanishes at about 1.2 eV. This corresponds to the energy at which the reflectivity in figure 2 exhibits a sharp drop and the energy-loss function (figure 6) also shows the first peak. This peak in energy-loss function at about 1.2 eV arises as  $\epsilon_1$  goes through zero and  $\epsilon_2$  is small at such energy, thus fulfilling the condition for plasma resonance at 1.2 eV ( $\hbar\omega_p = 1.2$  eV). The loss function has other peaks at higher energies which could arise due to interband transitions. It is seen that the bands in figure 1, clustered between  $-7.0$  and  $1.0$  eV, exhibit a variety of features. It is known [23] that the bands that are close and parallel to the Fermi level give rise to bumps of interband transitions at low energies, the bands that are parallel in a significant part of the Brillouin zone give rise to peaks at higher energies while the bands that are degenerate or close at one point and then separate from each other give rise to a near-constant number of



**Figure 2.** The calculated reflectivity of  $\text{MgCNi}_3$ .



**Figure 3.** Calculated real and imaginary parts of the dielectric function of  $\text{MgCNi}_3$ .

transitions with a distinct onset of energy. Bands with these features are present in the band structure of  $\text{MgCNi}_3$ . Some of the Ni d bands are in fact quasi-parallel in a reasonable part of the Brillouin zone. Transitions in this region, or originating here, account for some of the peaks observed in the calculated reflectivity and energy-loss function.

In figures 4 and 5, the calculated absorption coefficient and real part of the optical conductivity are shown. The spectra have a lot of maxima and minima within the energy

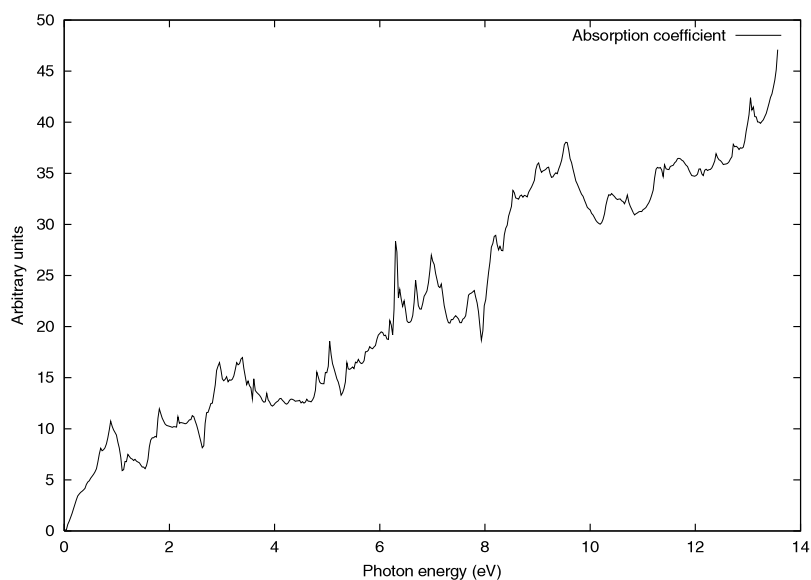


**Figure 4.** The calculated absorption coefficient of  $\text{MgCNi}_3$ .

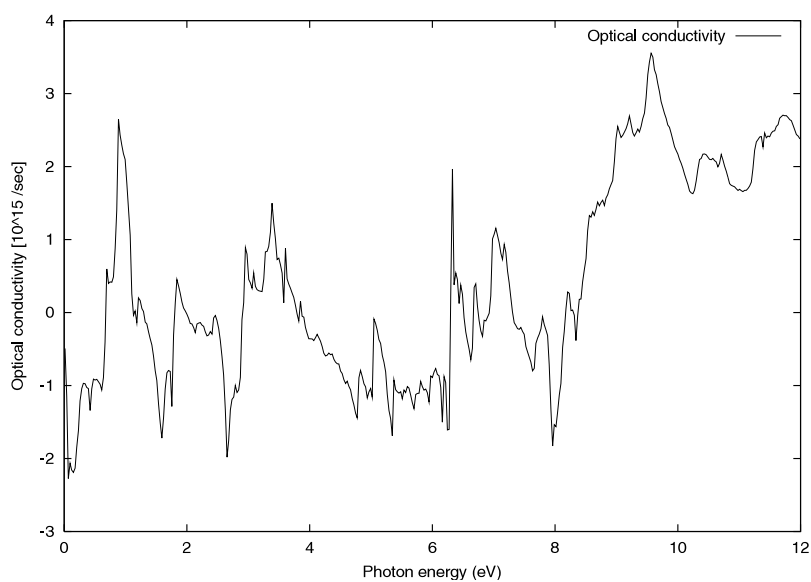


**Figure 5.** The calculated real part of the optical conductivity of  $\text{MgCNi}_3$ .

range studied. The peak structures can be explained from the interband transitions using our band structure results. The peaks in figures 4 and 5, within the energy range 0–8.0 eV, can be attributed to the interband transitions from the quasi-parallel Ni 3d bands clustered between  $-4.0$  eV and the Fermi level, and from the C 2s/Ni 3d band at about 3.0 eV between the  $\Delta$  point, through the  $\Delta$  point, to the  $\Gamma$  point in the Brillouin zone. The other peaks at higher energies may arise from transitions originating from various points on C 2p, C 2s bands lying between

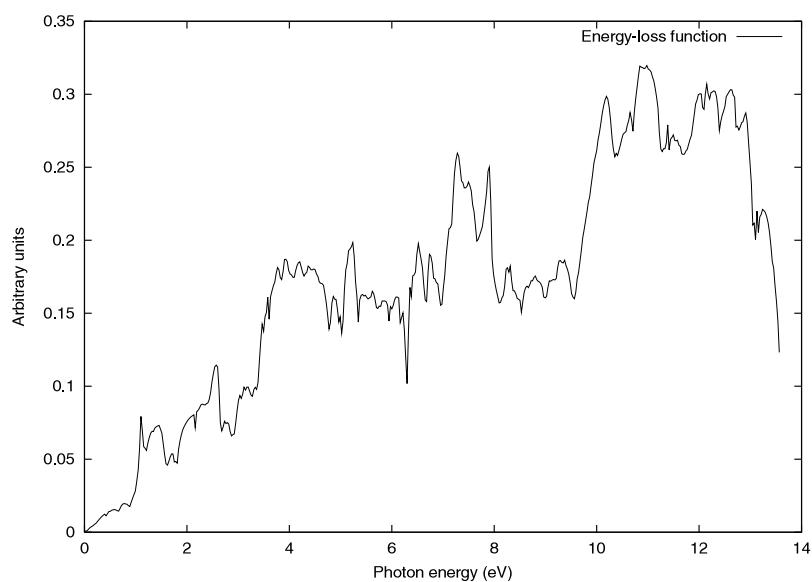


**Figure 6.** The calculated energy-loss spectrum of  $\text{MgCNi}_3$ .

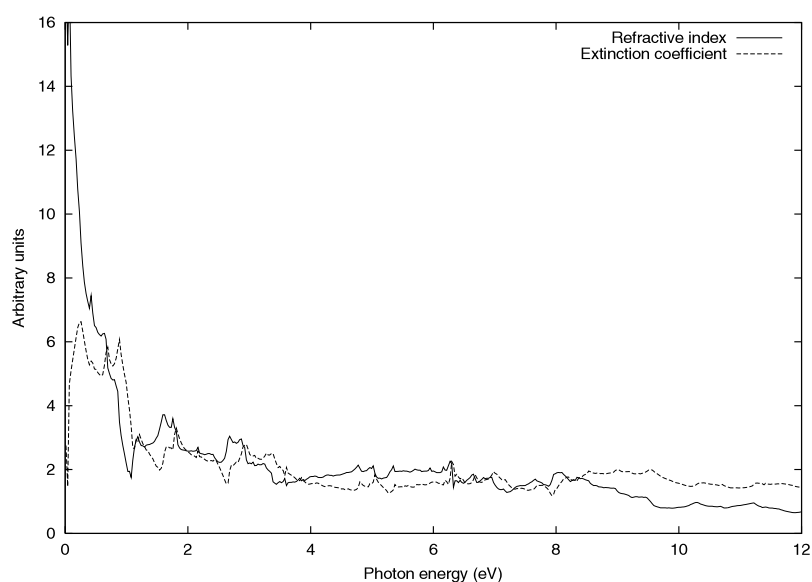


**Figure 7.** The calculated refractive index  $n(\omega)$  and extinction coefficient  $k(\omega)$  of  $\text{MgCNi}_3$ .

$-7.0 \rightarrow -4.0$ ,  $-13.0 \rightarrow -11.0$  eV respectively to the C 2s/Ni 3d band around 3.0 eV. These transitions could have implications for the understanding of superconductivity in  $\text{MgCNi}_3$ . Finally, figure 7 shows the dependence of the refractive index and extinction coefficient on energy for the superconducting antiperovskite  $\text{MgCNi}_3$ . The interband transitions discussed above also explain the origin of the peak structures in the refractive index and the extinction coefficient. It is pertinent to note, however, that the theoretically calculated spectra of optical



functions depend on the accuracy of the method and, since it is well known that density functional theory is, in principle, exact for ground state properties, we think that some structures in the optical spectra may well have their origin in the method via the local exchange–correlation potential employed. Furthermore, the inadequacy of density functional theory to account for excited states could also lead to wrongly predicted positions of peaks. On the whole, it is possible that superconductivity in  $\text{MgCNi}_3$  originates from the interaction between Ni 3d and C 2p states. To the best of our knowledge, there is no experimental result on the optical properties of  $\text{MgCNi}_3$ ; we therefore hope that our calculations will motivate experimental studies in this direction. Availability of experimental data will help in making quantitative comparisons with theoretical results.

#### 4. Conclusions

In conclusion, we have carried out a detailed investigation of the optical properties of the antiperovskite  $\text{MgCNi}_3$  using the FP-LAPW method. We have calculated the dielectric function, reflectivity, absorption coefficients, optical conductivity, energy-loss function, refractive index and extinction coefficient. Using the band structure, we have discussed the origin of the features that appear in the optical properties. The calculated reflectivity spectra predict large reflectivity in the low-energy region. On the whole, our results for the optical properties await experimental findings for comparison.

#### Acknowledgments

The author would like to thank Professor P Blaha and his group for allowing the use of the WIEN97 code. My thanks also go to the International Atomic Energy Agency and UNESCO for hospitality at the Abdus Salam International Centre for Theoretical Physics (ICTP), Trieste, Italy. Financial support of the Swedish International Development Cooperation Agency (SIDA) during my visit to ICTP as a regular associate is acknowledged.

#### References

- [1] He T, Huang T Q, Ramirez A P, Wang Y, Regan K A, Rogado N, Hayward M A, Haas M K, Slusky J S, Inumaru K, Zandbergen H W, Ong N P and Cava R J 2001 *Nature* **411** 54
- [2] Huang Q, He T, Regan K A, Rogado N, Hayward M, Haas M K, Inumaru K and Cava R G 2001 *Preprint cond-mat/0105240*
- [3] Hayward M A, Haas M K, Ramirez A P, He T, Regan K A, Rogado N, Inumaru K and Cava R J 2001 *Solid State Commun.* **119** 491
- [4] Papaconstantopoulos D A and Pickett W E 1992 *Phys. Rev. B* **45** 4008  
Vansant P R, Van Camp P E, Van Doren V E and Martins J L 1998 *Phys. Rev. B* **57** 7615
- [5] Shim J H and Min B I 2001 *Phys. Rev. B* **64** 180510
- [6] Dugdale S B and Jarlborg T 2001 *Phys. Rev. B* **64** 100508
- [7] Szajek A 2001 *J. Phys.: Condens. Matter* **13** L595
- [8] Singh D J and Mazin I I 2001 *Phys. Rev. B* **64** 140507
- [9] Rosner H, Weht R, Johannes M D, Pickett W E and Tosatti E 2002 *Phys. Rev. Lett.* **88** 027001
- [10] Wang Y X, Zhong W L, Wang C L and Zhang P L 2001 *Solid State Commun.* **120** 133
- [11] Wang Y X, Zhong W L, Wang C L and Zhang P L 2001 *Phys. Lett. A* **120** 133
- [12] Wang Y X, Zhong W L, Wang C L and Zhang P L 2001 *Solid State Commun.* **120** 137
- [13] Saha S, Sinha T P and Mookerjee A 2000 *Phys. Rev. B* **62** 8828
- [14] Saha S, Sinha T P and Mookerjee A 2000 *J. Phys.: Condens. Matter* **12** 3325
- [15] Saha S, Sinha T P and Mookerjee A 2000 *Eur. Phys. J. B* **18** 207
- [16] Blaha P, Schwarz K and Luitz J 1997 *WIEN97, a Full Potential Linearized Augmented Plane Wave Package for Calculating Crystal Properties* Technical University of Vienna (ISBN 3-9501031-0-4)

- This is an improved and updated Unix version of the original copyrighted WIENcode, which was published by Blaha P, Schwarz K, Sorantin P and Trickey S B 1990 *Comput. Phys. Commun.* **59** 399
- [17] Singh D J 1994 *Planewaves, Pseudopotentials and the LAPW Method* (Boston, MA: Kluwer)
  - [18] Hohenberg P and Kohn W 1964 *Phys. Rev.* **136** 864
  - [19] Kohn W and Sham L J 1965 *Phys. Rev. A* **140** 1133
  - [20] Perdew J P, Burke S and Ernzerhof M 1996 *Phys. Rev. Lett.* **77** 3865  
Perdew J P, Burke S and Ernzerhof M 1997 *Phys. Rev. Lett.* **78** 1396 (erratum)
  - [21] Ambrosch-Draxl C and Abt R 1998 *The Calculation of Optical Properties within WIEN97* ICTP Lecture Notes (unpublished)
  - [22] Yu Y P and Cardona M 1999 *Fundamentals of Semiconductors: Physics and Materials Properties* 2nd edn (Berlin: Springer) p 241
  - [23] Fox M 2001 *Optical Properties of Solids* (New York: Oxford University Press) p 6
  - [24] Delin A, Eriksson A O, Ahuja R, Johansson B, Brooks M S S, Gasche T, Auluck S and Wills J M 1996 *Phys. Rev. B* **54** 1673
  - [25] Murnaghan F D 1994 *Proc. Natl Acad. Sci.* **30** 244